Nuclear Engineering and Technology 50 (2018) 453–461

Contents lists available at ScienceDirect

Nuclear Engineering and Technology

journal homepage: www.elsevier.com/locate/net

Original Article

# Analysis of queuing mine-cars affecting shaft station radon concentrations in Quzhou uranium mine, eastern China

Changshou Hong [a, *], Guoyan Zhao [a], Xiangyang Li [b]

[a] School of Resources and Safety Engineering, Central South University, Changsha 410083, China
[b] School of Environmental and Safety Engineering, University of South China, Hengyang 421001, China

ARTICLE INFO

*Article history:*
Received 28 November 2016
Received in revised form
2 November 2017
Accepted 17 November 2017
Available online 7 December 2017

*Keywords:*
Hoist and Transport Systems
Mine-cars
Queuing Simulation
Radon Concentration
Underground Uranium Mine

ABSTRACT

Shaft stations of underground uranium mines in China are not only utilized as waiting space for loaded mine-cars queuing to be hoisted but also as the principal channel for fresh air taken to working places. Therefore, assessment of how mine-car queuing processes affect shaft station radon concentration was carried out. Queuing network of mine-cars has been analyzed in an underground uranium mine, located in Quzhou, Zhejiang province of Eastern China. On the basis of mathematical analysis of the queue network, a MATLAB-based quasi-random number generating program utilizing Monte-Carlo methods was worked out. Extensive simulations were then implemented via MATALB operating on a DELL PC. Thereafter, theoretical calculations and field measurements of shaft station radon concentrations for several working conditions were performed. The queuing performance measures of interest, like average queuing length and waiting time, were found to be significantly affected by the utilization rate (positively correlated). However, even with respect to the "worst case", the shaft station radon concentration was always lower than 200 Bq/m$^3$. The model predictions were compared with the measuring results, and a satisfactory agreement was noted. Under current working conditions, queuing-induced variations of shaft station radon concentration of the study mine are not remarkable.



## 1. Introduction

Radon, as a decay product emanating from the earth's crust, is the unique naturally occurring radioactive noble gas, without any color, odor, or taste. Radon and its progenies have been acknowledged as the secondary most important cause of lung cancer after heavy smoking [1,2]. It is well known that a common occurrence of radiological hazard in uranium mines is inhalation of radon and its progenies [3]. Numerous studies have been concerned with analyses of radon sources and factors affecting radon exhalation in underground uranium mines [4–7]. As to underground uranium mines employing exhaust ventilation systems, shaft stations are the major air inlets. Yet, few analytic or numerical studies have looked at assessing the effects of queuing of mine-cars on elevated radon concentration.

During a normal mining period in most underground uranium mines in China, successive streams of fully-loaded mine-cars are hauled to a shaft station and subsequently hoisted via a hoist system to the ground surface. From the viewpoint of queuing theory, arrival flow is in general used to describe the hauling process and service flow the hoisting process. Inevitably there should always be a stochastic number of mine-cars queuing in a shaft station and waiting for service, while the awaiting mine-cars should be fully loaded with uranium ore piles.

The uranium ore piles are one of the major radon sources in underground uranium mines; radon exhalations can contribute to elevated radon concentrations in confined spaces like roadways and stopes [4,7]. In knowledge of this, shaft station radon concentration is prescribed at not above 200 Bq/m$^3$ [8]. This article is an analysis of mine-car queuing processes, performed via simulation method; in-depth estimation is also performed of queuing process effects on shaft station radon concentration.

* *Corresponding author.*
E-mail address: hongchangshou@163.com (C. Hong).

https://doi.org/10.1016/j.net.2017.11.008

## 2. Case study mine

This study was carried out in the Quzhou uranium mine; the mine is located at the Jiangshan-Shaoxing fault zone in the eastern part of China. Fig. 1 shows the location of the case study mine and the different lithological units around it. The mineral compositions of uranium ore are primarily comprised of uraninite and coffinite; uranophane, uranopilite, and autunite are ascertained as the most common secondary minerals. Some other essential minerals are quartz, calcite, fluorite, and mica. Detailed descriptions of the mineralization and geologic features of this mine have previously been made by Mao [9,10]. The grade and porosity of the uranium ore are 0.11% and 2.5%, respectively.

The Quzhou uranium mine is opened up by a vertical shaft; therein, at −15 m level is the study area of the investigated mine. The vertical shaft is for ore-hoisting and air inlet uses only; the shaft station at −15 m level is designed as loop-type. Mine-cars are utilized in the underground transport system and a cage in the hoist system. Carrying capacity of the cage is at most two mine-cars per hoist cycle. The hoist and transport systems of this mine are schematically presented in Fig. 2.

## 3. Methods

### 3.1. Queuing model

The mine-car queuing processes are shown in Fig. 3. Notice that the loaded track is the crucial node for the mine-cars queuing network because of its dual role as waiting space for loaded mine-cars queuing to be hoisted as well as channel for air inlet. Thus, we select this part of the shaft station as the key research object; for

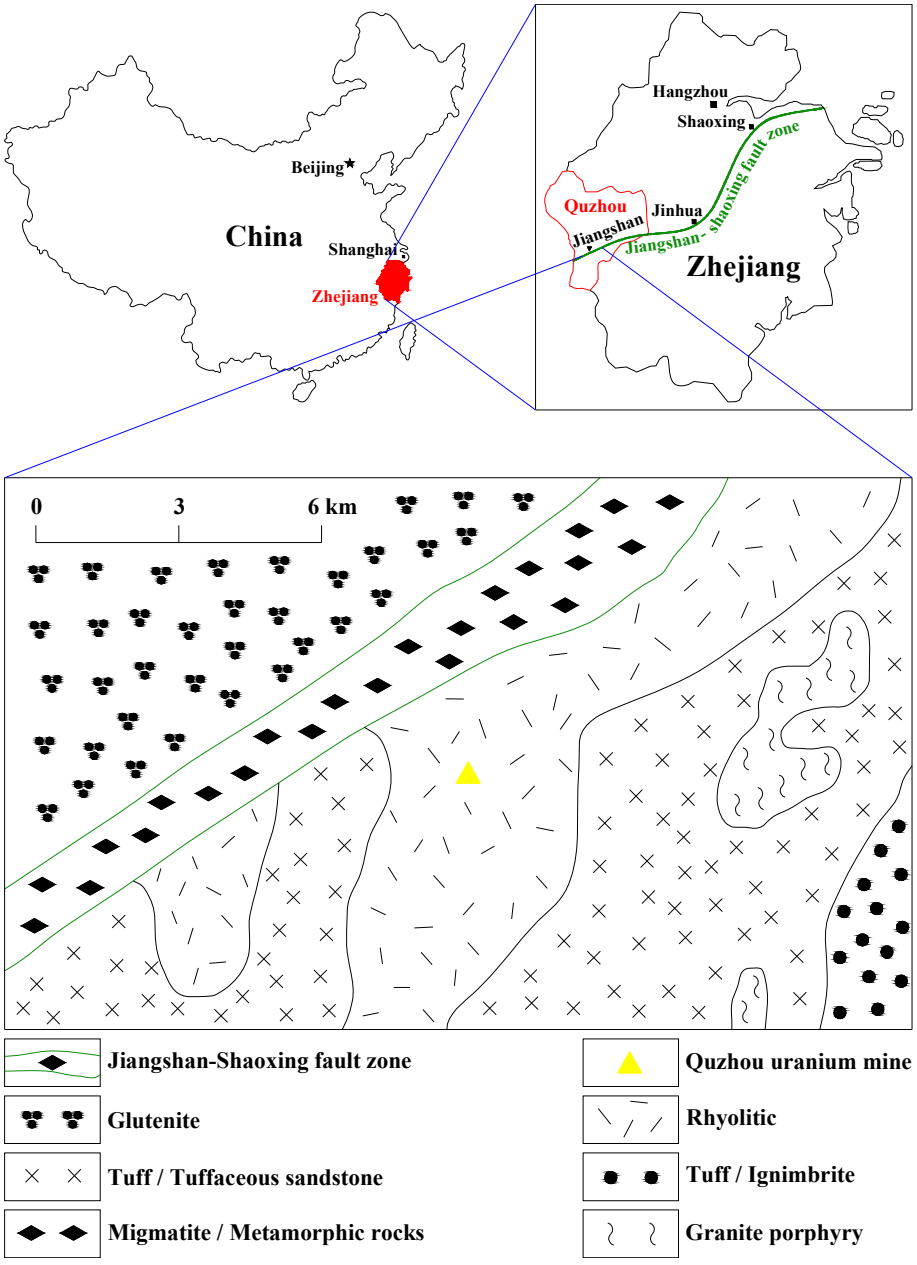


**Fig. 1.** The location and lithological units of Quzhou uranium mine.

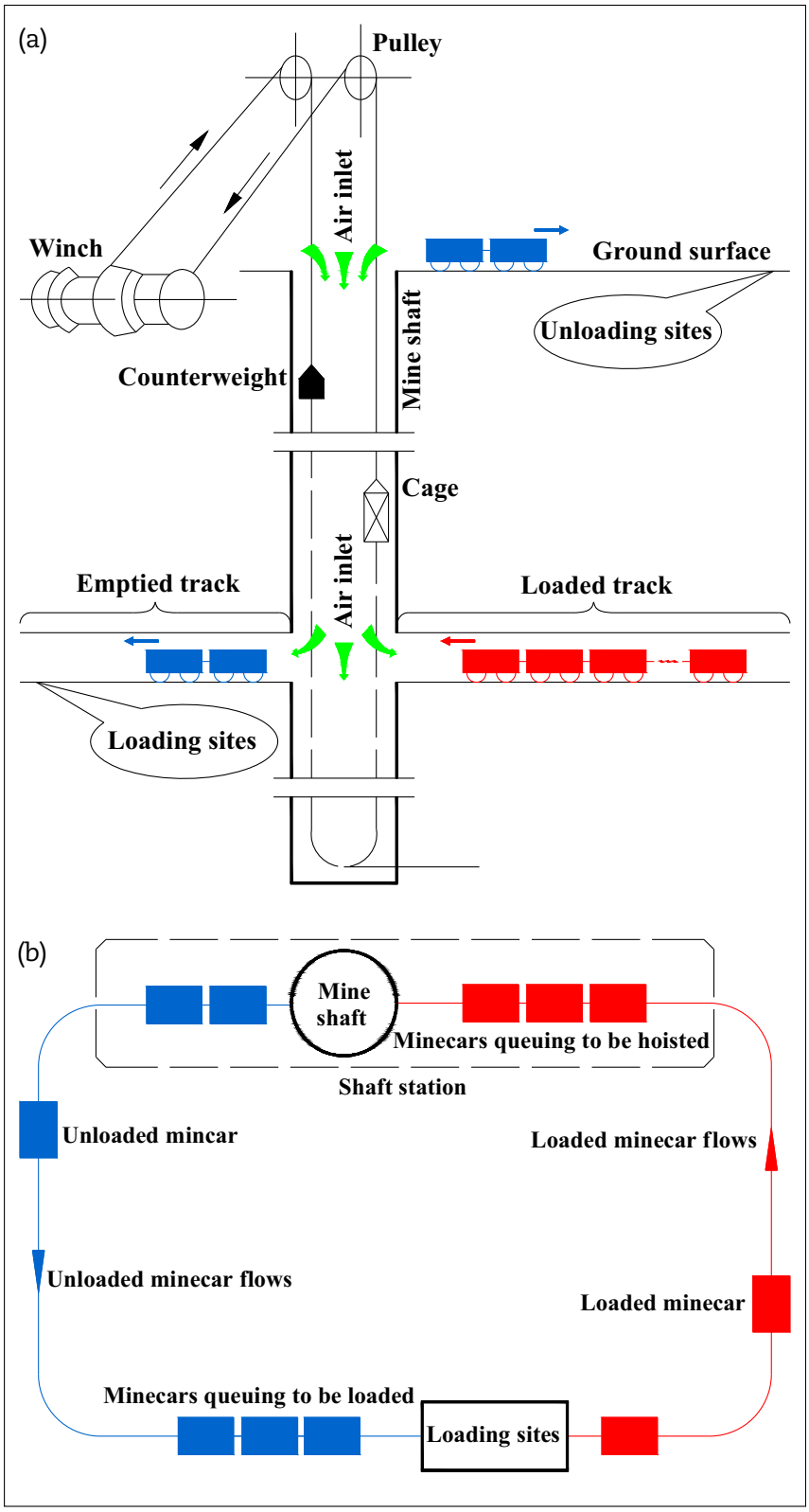


**Fig. 2.** Schematic presentations of the hoist and transport systems of Quzhou uranium mine. (A) Vertical cross-section. (B) Horizontal cross-section of −15 m level and mine-cars queuing network.

convenient discussion, "shaft station" is still used to represent the loaded track throughout the present study.

As shown in Fig. 3, the mine-cars queuing network has single input and output paths, namely the loaded track and emptied track, respectively. The cage equipped in the vertical shaft acts as the only server and is applied to convey loaded mine-cars up to the pithead and unloaded ones down to the −15 m level. Several characteristics of the mine-car queuing network are as follows:

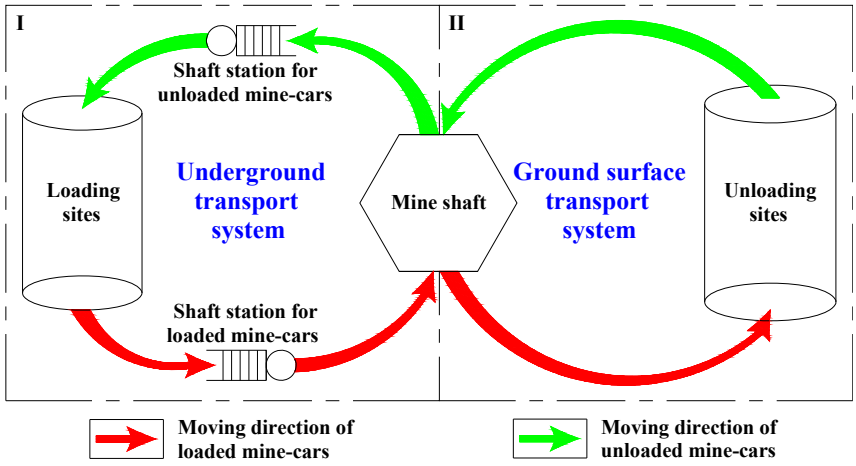


**Fig. 3.** Mine cars queuing network: I—underground part; II—ground surface part.

- Finite customers with total 120 mine-cars in closed cycle, and each customer consists of two mine-cars.
- Finite waiting space with total 32 customers (or 64 mine-cars) due to limited dimensions of the shaft station.
- Following the scheduling of first come first service [11].
- Batched arrivals (with four pairs of mine-cars every time, namely four customers each arrival) in exponentially distributed time intervals [12].
- Services (with one pair of mine-cars every time, namely one customer each service) in exponentially distributed time intervals [12].
- No arrivals (or services) when the waiting space (or the server) is occupied.
- Considering the mining operation to be continuous (namely an uninterrupted queue), the initial moment 0 (unit: min) and no arrival, waiting, or service in the initial moment.

The arrival moment ($T_{a(i)}$, min) of customers in the queue, which means the moment of the $i^{th}$ batch of customers arriving at the shaft station, is defined as:

$$T_{a(i)} = T_{a(i-1)} + X_{(i)} \quad i = 1, 2, \cdots, n \tag{1}$$

where $n$ is a positive integer that represents the frequency of arrivals, and $X_{(i)}$ is a random number that indicates the time interval between the $i^{th}$ and the $(i-1)^{th}$ batch arrivals (min). The interarrival time $X_{(i)}$ (the set of $X_{(i)}$ is denoted as $X = \{x | x = X_{(1)}, X_{(2)}, \ldots, X_{(i)}\}$), as a result of being considered as a queuing network exhibiting exponentially distributed arrival times, obeys the following exponential probability distribution function with parameter $\lambda$ [13–15]:

$$f(x) = \begin{cases} \lambda e^{-\lambda x} & \text{if } x \geq 0; \\ 0 \text{ otherwise.} \end{cases} \tag{2}$$

where $\lambda$ is the pseudo-arrival rate ($min^{-1}$). The expected interarrival time $X_{(i)}$ is $E(X_{(i)}) = 1/\lambda$ (min); thus, the actual arrival rate is:

$$\lambda^* = \frac{4}{E\left(X_{(i)}\right)} = 4\lambda \tag{3}$$

where $\lambda^*$ is the actual arrival rate ($min^{-1}$).

The service moment ($T_{s(j)}$, min) of a customer in the queue, which means the moment of the $j^{th}$ customer being in service via the cage, is defined as:

$$T_{s(j)} = \begin{cases} \max\left\{T_{s(j-1)} + Y_{(j)}, T_{a(i)}\right\} & \text{if } j = (4i-3); \\ T_{s(j-1)} + Y_{(j)} & \text{if } j = (4i-2), j = (4i-1) \text{or } j = 4i. \end{cases} \tag{4}$$

where $Y_{(j)}$ is random number that means the time interval between the $j^{th}$ and the $(j-1)^{th}$ services (min). The interservice $Y_{(j)}$ (the set of $Y_{(j)}$ is denoted as $Y = \{y | y = Y_{(1)}, Y_{(2)}, \ldots, Y_{(j)}\}$), due to the impossibility of $Y_{(j)} = 0$, obeys the following shifted exponential probability distribution function with parameters $\mu$ and $Y_0$:

$$f(y) = \begin{cases} \mu e^{-\mu(y-Y_0)} & \text{if } y \geq Y_0; \\ 0 \text{ otherwise.} \end{cases} \tag{5}$$

where $\mu$ is the pseudo-service rate ($min^{-1}$), and $Y_0$ is the minimum interservice time. The expected interservice time $Y_{(j)}$ is $E(Y_{(j)}) = Y_0 + 1/\mu$ (min); thus, the actual service rate is:

$$\mu^* = \frac{1}{E\left(Y_{(j)}\right)} = \frac{\mu}{\mu Y_0 + 1} \tag{6}$$

where $\mu^*$ is the actual service rate ($min^{-1}$).

The waiting time ($W_{q(j)}$, min) of a customer in the queue, which means the waiting time of the $j^{th}$ customer at the shaft station, is defined as:

$$W_{q(j)} = T_{s(j)} - T_{a(i)} \tag{7}$$

Queuing performance measures, like average queuing length ($\overline{L}_q$, customer) and average waiting time ($\overline{W}_q$, min), are of our interest in evaluating the shaft station radon concentration; therefore, we gave their computational formulas in the following.

The average waiting time ($\overline{W}_q$) of customers in the queue can be estimated by [16]:

$$\overline{W}_q = \sum_{j=1}^{4n} \frac{W_{q(j)}}{4n} \tag{8}$$

The average queuing length ($\overline{L}_q$, customer) of customers in the queue can be determined by [16]:

$$\overline{L}_q = \overline{W}_q \Big/ \left(\frac{T_{s(4n)}}{4n}\right) = \sum_{j=1}^{4n} \frac{W_{q(j)}}{T_{s(4n)}} \tag{9}$$

The utilization rate ($\rho$) of the server, which is the ratio of arrival rate to service rate, is invariably less than 1 or else leads to an overflowing queue [17,18] and is determined by:

$$\rho = \frac{\lambda^*}{\mu^*} = 4\lambda\left(Y_0 + \frac{1}{\mu}\right) \tag{10}$$

### 3.2. Monte-Carlo simulation

Monte-Carlo methods (MC methods) are commonly utilized and widely accepted as statistical testing techniques that depend on repeated random sampling to obtain approximate solutions of various discrete event systems [19–21]. Note that, it is almost impossible to obtain the precise solutions of $\overline{W}_q$ and $\overline{L}_q$; therefore, an MC simulation was conducted. The MATLAB program, used as a quasi-random number generator, was developed to conduct the MC simulations; the flowchart of the program is shown in Fig. 4.

The input parameters that were utilized in the MC simulations include the pseudo-arrival rate ($\lambda$), the pseudo-service rate ($\mu$) and the minimum interservice time ($Y_0$), where the latter two parameters are closely associated with the annual capacity of uranium ore

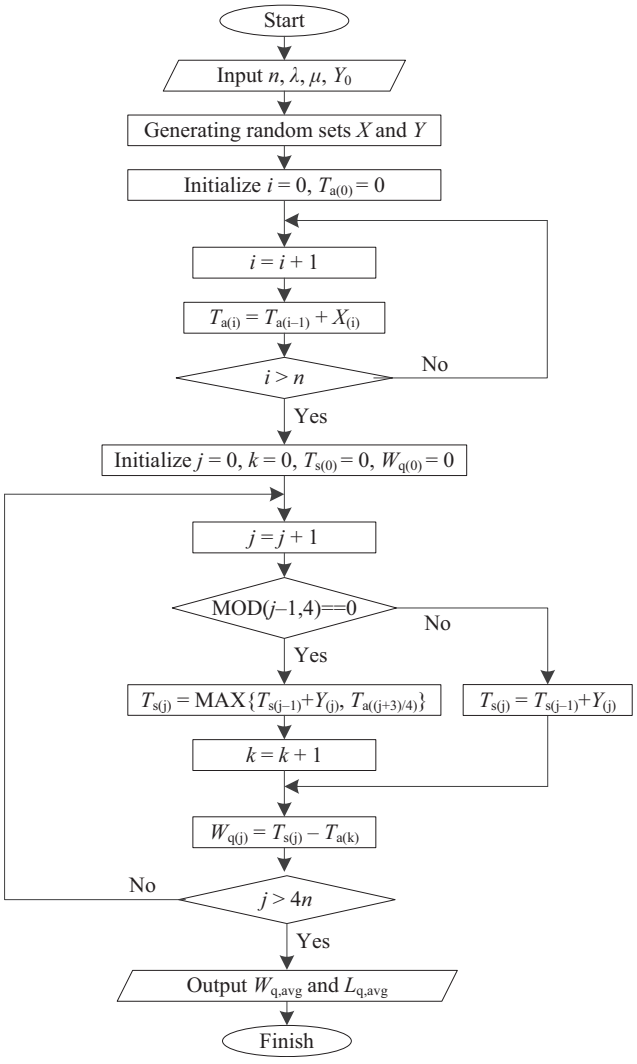


**Fig. 4.** Flowchart of the MATLAB program.

**Table 1**
Overview of the involved model parameters.

| Symbol | Description | Value (and unit) |
|---|---|---|
| $t_d$ | Working days per year | 330 d/yr |
| $t_h$ | Working hours per day | 16 hr/d |
| $K$ | Unbalance factor[a] | 1.2 |
| $M_0$ | Load capacity per mine-car | 1.375 tons |
| $Y_0$ | Minimum inter-service time | 3 min |

[a] It is a dimensionless constant that in general takes the value of 1.2 for cage dedicated for conveying ores [23].

hoisted via the cage. The annual capacity ($M_a$, tons/yr) is estimated by [22]:

$$M_a = \frac{t_d t_h M_h}{K} \tag{11}$$

where $t_d$ is working days per year (d/yr) and $t_h$ is the working hours per day (h/d), and $K$ is an unbalance factor that reflects the fluctuations of ore-hoisting capacity per unit time [23]; $M_h$ (tons/hr) is the hourly capacity of uranium ore piles hoisted via the cage and is formulated by:

$$M_h = \frac{\textit{Ore hoisting capacity per cage}(\text{tons}) \times 60(\text{min/hr})}{\textit{Expected inter} - \textit{service time}(\text{min})} = \frac{120\mu M_0}{\mu Y_0 + 1} \tag{12}$$

where $M_0$ is the load capacity per mine-car. In particular, the ore-hoisting capacity per cage is twice the load capacity per mine-car.

By combining Eqs. (10)–(12), we obtain:

$$M_a = \frac{480\lambda t_d t_h}{\rho K} \cdot M_0 \tag{13}$$

In China, the allowable limit of annual capacity for a cage is 100,000 tons/yr [8]. For a "worst case" study, we assume that $M_a$ = 100,000 tons/yr. An overview of the involved model parameters is given in Table 1.

Substituting corresponding parameter values into Eq. (13), it becomes:

$$\rho = 29.04\lambda \tag{14}$$

Moreover, from Eqs. (10) and (14) we can obtain the value of the pseudo-service rate ($\mu$), namely $\mu$ = 0.2347.

## 4. Results and discussion

### 4.1. Simulation results

Notice that the input parameter values have been obtained, except for the pseudo-arrival rate ($\lambda$), which is positively associated with the utilization rate ($\rho$), as indicated by Eq. (14); Therefore, we aim to explore, through MC simulations, how the output parameters, namely average waiting time ($\overline{W}_q$) and average queuing length ($\overline{L}_q$), are affected by modifying the utilization rate ($\rho$). We implemented all the MC simulations using a Dell INSPIRON 1420 with a dual core and a 32-bit Core 2 Duo-T5800 2.00 GHz processor running on Windows 7. To produce good approximate solutions, we performed 1,000,000 iterations for each simulation (simulation unit of step size: $\Delta h_\rho$ = 0.03), with a total of 10 simulations. The simulation results are shown in Figs. 5 and 6.

Figs. 5 and 6 respectively show how the average queuing length ($\overline{L}_q$) and average waiting time ($\overline{W}_q$) of customers are

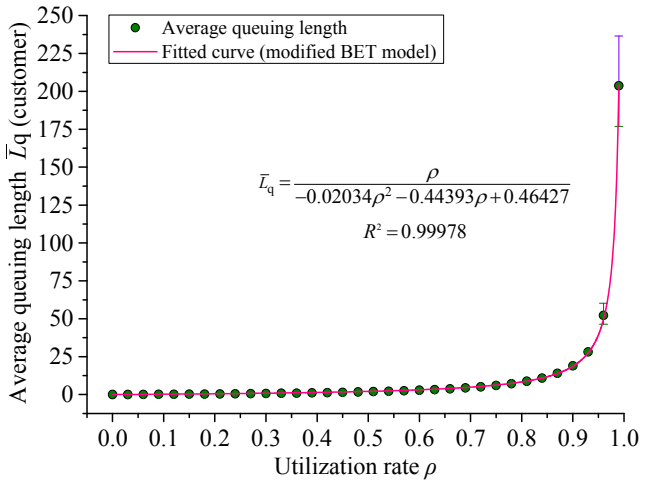


**Fig. 5.** Average queuing length ($\bar{L}_q$) of customers in the queue in function of utilization rate ($\rho$).

affected by increasing the utilization rate ($\rho$); the obtained values match well with those of modified Brunauer–Emmett–Teller (BET) models. Increasing utilization rate in the interval of $\rho \in [0,0.9]$ has a relatively insignificant impact on the increase of the average queuing length and average waiting time of customers. However, the two parameters increase sharply when $\rho$ is higher than 0.9 or so. Furthermore, allowing for the fact that the peak of customers in the shaft station would not be above 32 (denoted as $\bar{L}_{q,max} = 32$), the ultrautilization rate is 0.9393 (denoted as $\rho_{max} = 0.9393$), obtained by solving the fitted equation shown in Fig. 5. Then, substituting $\rho_{max} = 0.9393$ into the fitted equation shown in Fig. 6, we determined that the peak of average waiting time ($\overline{W}_q$) is 246.4584 min (denoted as $\overline{W}_{q,max} = 246.4584$ min).

### 4.2. Shaft station radon concentration

The results obtained from the MC simulations indicate that variations of the number of mine-cars (namely $\bar{L}_q$) and their waiting times ($\overline{W}_q$) in the shaft station can be attributed to queuing processes with different utilization rates ($\rho$); apparently, the implications of the queuing processes mainly reflect (a) the changeable airflow rate of shaft station perturbed by the arrival and service flows and (b) the incremental shaft station radon concentration contributed to by the uranium ore piles loaded in the awaiting mine-cars. The details are described below.

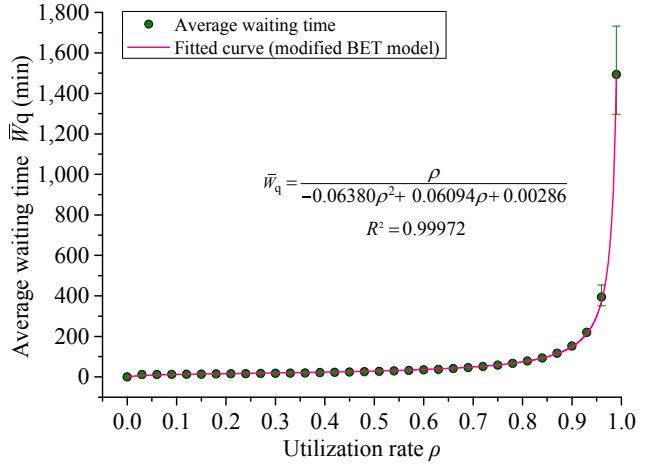


**Fig. 6.** Average waiting time ($\overline{W}_q$) of customers in the queue in function of utilization rate ($\rho$).

To evaluate the impact of the queuing processes on the airflow rate, we compared the air change rate of the shaft station with the actual arrival and actual service rates, as well as the reciprocal of the average waiting time, which represents the number of customers per minute waiting in the shaft station. According to Eqs. (3), (10), and (14), we obtained the actual arrival rate ($\lambda^*$): $\lambda^* = (0.1377\rho)$ min$^{-1}$; and the actual service rate ($\mu^*$): $\mu^* = 0.1377$ min$^{-1}$. The air change rate can be expressed as:

$$\eta = \frac{60q}{V} \tag{15}$$

where $\eta$ is the air change rate of the shaft station (min$^{-1}$), $q$ is the airflow rate of the shaft station (m$^3$/s), $V$ is the effective volume of the shaft station expressed as $V=(SL-N_cV_c)$ (m$^3$), $S$ is the cross-sectional area of the shaft station (m$^2$), $L$ is the length of the shaft station (m), $V_c$ is the volume of the mine-car (m$^3$), $N_c$ is the number of waiting mine-cars in the shaft station, namely the average queuing length and $N_c$ is equal to $2\bar{L}_q$ ($\bar{L}_q$ vs. $\rho$ see Fig. 5). By substituting the corresponding parameter values (see Table 2) into Eq. (15) and combining the fitted equation shown in Fig. 6, the comparisons of $\eta$ with $\lambda^*$, $\mu^*$ as well as $(1/\overline{W}_q)$ are schematically shown in Fig. 7.

All the results (y-axis) are in units of time (min$^{-1}$), so no detailed descriptions of Y-labels were placed in Fig. 7. In this figure, we see that on most occasions the actual arrival and actual service rates as well as the reciprocal of the average waiting time are quite a bit smaller than the air change rate. Only when the utilization rate is in close proximity to zero, when there are hardly any customers waiting in the shaft station, the air change rate may be smaller than the reciprocal of the average waiting time. That is to say, the customer flows ascribed to queuing processes have little influence on the airflow rate. Hence, a steady-state model for the evaluation of the shaft station radon concentration was established upon some fundamental assumptions, which are listed in the following:

- All the cross-sections of the shaft station have the same area and perimeter.
- Radon sources only include inlet air, mine-walls, and uranium ore piles.
- Radon steadily exhales from the exposed surfaces of mine-walls and ore piles to shaft station airflow, and evenly mixes with it.
- Airflow carrying radon is in turbulent condition.

As provided in our previous study [24,25], the following calculation formula can be utilized in the evaluation of radon concentration at the back end of the shaft station, which is the place most probable to have the highest radon concentration:

$$C_{Rn,L} = C_{Rn,0} + \frac{J_w P_w L}{q} + \frac{N_c J_c S_c}{q} \tag{16}$$

where $C_{Rn,L}$ represents radon concentration at the back end of the shaft station (Bq/m$^3$). The terms on the right-hand side of Eq. (16) indicate the elevated radon concentrations at the back end of the shaft station contributed by inlet air, mine-walls, and mine-cars, respectively. We hereby define the ratio of the elevated radon concentration (namely $C_{Rn,0}$, $J_wP_wL/q$ or $N_cJ_cS_c/q$) to the radon concentration at the back end of the shaft station (namely $C_{Rn,L}$) as

**Table 2**
Parameters along with their values.

| Symbol | Description | Value (and unit) |
|---|---|---|
| $C_{Rn,0}$ | Initial radon concentration of the inlet air | 64.8 Bq/m$^3$ |
| $q$ | Airflow rate in the shaft station | 12.3 m$^3$/s |
| $S$ | Cross-sectional area of the shaft station | 10.9 m$^2$ |
| $L$ | Length of the shaft station | 105.2 m |
| $L_c$ | Length of the mine-car | 1.6 m |
| $N_c$ | The number of awaiting mine-cars[a] | $2\overline{L}_q$ |
| $V_c$ | Volume of the mine-car | 1.8 m$^3$ |
| $V$ | Effective volume of the shaft station | $(1146.68-3.6\overline{L}_q)$ m$^3$ |
| $S_c$ | Expose area of the mine-car | 1.5 m$^2$ |
| $J_c$ | Radon exhalation rate of the uranium ore piles[b] | $47.79\times10^{-3}$ Bq/(m$^2$·s) |
| $P_w$ | Perimeter of the shaft station cross-section | 12.6 m |
| $J_w$ | Radon exhalation rate of the mine-walls[b] | $11.54\times10^{-3}$ Bq/(m$^2$·s) |

[a] Namely the average queuing length, and $N_c$ is equal to $2\overline{L}_q$ (see Fig. 5).
[b] They are the average of field measured data by the methods provided by Sahu et al. [5].

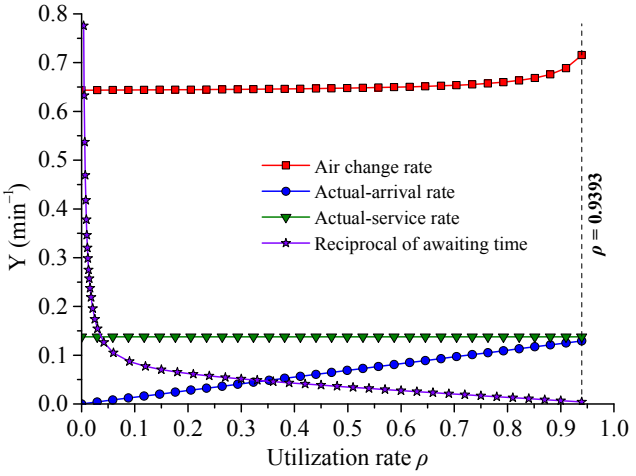


**Fig. 7.** Comparisons of air change rate with actual arrival and actual service rates and the reciprocal of waiting time.

the contribution rate, and the sign $\delta$ denotes the contribution rate of uranium ore piles loaded in the awaiting mine-cars and is determined by:

$$\delta = \frac{N_c J_c S_c}{q C_{Rn,L}} \tag{17}$$

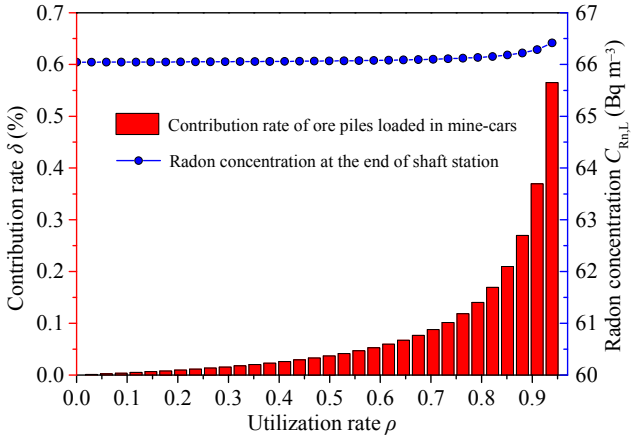


**Fig. 8.** Effect of utilization rate on radon concentration at the back end of shaft station along with contribution rate of uranium ore piles loaded in mine-cars.

Substituting the involved parameter values into Eq. (17), the effect of $\rho$ on $\delta$, along with its effect on $C_{Rn,L}$, can be schematically shown as in Fig. 8.

Fig. 8 shows that the utilization rate has a weak impact on the radon concentration at the back end of the shaft station; uranium ore piles loaded in the awaiting mine-cars contribute little, comprising within the maximal contribution rate $\delta_{max}$ less than 0.6%, to the elevated shaft station radon concentration under the current conditions. That is to say, radon contained in inlet air and radon exhalation from mine-walls are the major radon sources; queuing processes make little difference.

### 4.3. Discussion

To demonstrate the validity of the proposed model along with the methods utilized in the model, we carried out eight frequently-seen cases of field measurements of queuing parameters and shaft station radon concentration in the study area, taking 16 h as a single measurement cycle. Several measured and derived parameters for the queuing model are summarized in Table 3.

Assuming that the queuing model and MC methods are valid, we implemented the MC simulations (still 1,000,000 iterations for each simulation and a total of 10 simulations) for the eight cases with the parameters shown in Table 3. The simulation results, along with the field monitoring data of average queuing length ($\overline{L}_q$) and average waiting time ($\overline{W}_q$), are shown in Fig. 9. Moreover, RAD7 radon monitors (DURRIDGE Corp., Billerica, Massachusetts, USA) were utilized to measure the real-time radon concentrations at both ends of the shaft station. Settings of the monitors were (1) purging for 5 min before starting a measurement; (2) selecting a period of 10 min for a single measurement cycle; (3) adopting "sniff" mode; and (4) pump setting as "auto" mode. Additionally, we employed a TSI9565 digital anemometer (TSI Corp., Shoreview, Minnesota, USA) to monitor the airflow rate at the back end of the shaft station for each case. The measured data of radon concentration at both ends of the shaft station and airflow rates at the back end of the shaft station, along with the simulation results derived using our developed model, are shown in Fig. 10.

In Fig. 9, we can see that the simulation results of average queuing length, as well as average waiting time, show trends highly similar to the data obtained by field measurements. Particularly, for almost all cases, the simulation results are within the range of the measured results. As can be seen in Fig. 10, though the tendencies of the measured and simulation results of radon concentration at the back end of the shaft station have a rough degree of similarity,

**Table 3**
Measured and derived parameters for queuing model.

| Case | Arrivals[a] | Services[a] | Arrival rate ($min^{-1}$)[b] | | Service rate ($min^{-1}$)[b] | | Utilization rate[c] |
|---|---|---|---|---|---|---|---|
| | | | Actual | Pseudo | Actual | Pseudo | |
| 1 | 38 | 237 | 0.1583 | 0.0396 | 0.2469 | 0.9522 | 0.6412 |
| 2 | 31 | 149 | 0.1292 | 0.0323 | 0.1552 | 0.2904 | 0.8325 |
| 3 | 54 | 273 | 0.2250 | 0.0563 | 0.2845 | 1.9420 | 0.7909 |
| 4 | 46 | 312 | 0.1917 | 0.0479 | 0.3250 | 13.0000 | 0.5898 |
| 5 | 32 | 241 | 0.1333 | 0.0333 | 0.2510 | 1.0162 | 0.5311 |
| 6 | 70 | 305 | 0.2917 | 0.0729 | 0.3177 | 6.7740 | 0.9182 |
| 7 | 40 | 184 | 0.1667 | 0.0417 | 0.1917 | 0.4512 | 0.8696 |
| 8 | 22 | 210 | 0.0917 | 0.0229 | 0.2188 | 0.6368 | 0.4191 |

[a] The arrivals and services represent the total number of customers' inter-arrivals and -services during a single measurement cycle, respectively.
[b] The actual arrival rate or actual service rate is equal to the ratio of arrivals or services to measurement period, and the pseudo-arrival and service rates are derived by utilizing Eqs. (3) and (6), respectively.
[c] The utilization rates are obtained by using Eq. (10).

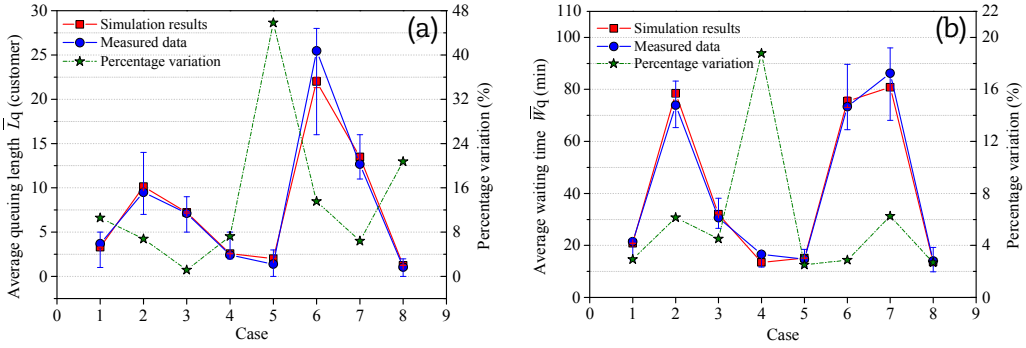


**Fig. 9.** Comparison of measured data with simulation results of queuing performance measures. (A) Average queuing length ($\overline{L}_q$). (B) Average waiting time ($\overline{W}_q$).

careful comparisons show that the simulation results still vary in the range of the measured results.

## 5. Conclusions

Mine-cars in queuing processes have little impact on the fluctuations of shaft station airflow rate in the investigated underground uranium mine; even for the "worst case" (namely ultimate annual capacity $M_a$ = 100,000 tons/yr), queuing mine-cars make insignificantly positive contributions to the radon concentrations at the back end of the shaft station, which is the site most likely exposed to a high radon concentration. Field measurements of eight frequently-seen working conditions reveal that the shaft station radon concentration of the investigated underground uranium mine is generally without possibility of rising above 200 Bq/$m^3$; these results agree well with the theoretically calculated results. That is to say, the proposed model is valid; within the scope of the current conditions, there is no radon problem in the shaft station of this mine.

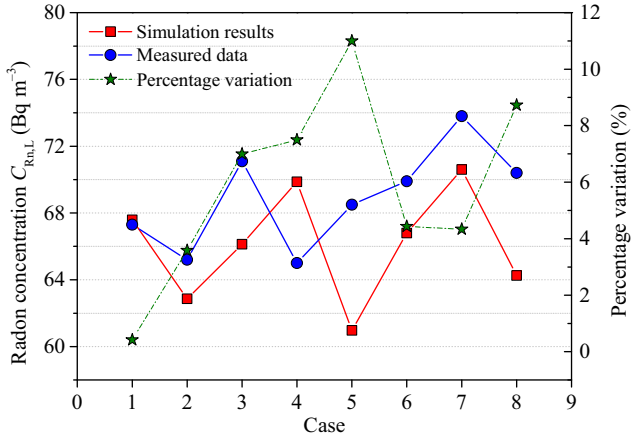


**Fig. 10.** Comparison of measured data with simulation results of radon concentration at the back end of shaft station.

### Conflicts of interest

All contributing authors declare no conflicts of interest.

### Acknowledgments

This work was supported by National Natural Science Foundation of China (NSFC) under funded projects N◌51374244 and N◌11475081, The authors wish to express thanks to NSFC.

### Appendix A. Supplementary data

Supplementary data related to this article can be found at https://doi.org/10.1016/j.net.2017.11.008.

### Appendix 1. Deduction of several parameters as shown in Figs. 7 and 8

By substituting the corresponding parameter values (see Table 2) into Eq. (15) and combining the fitted equation shown in Fig. 5, the Eq. (15) becomes:

$$\eta = \frac{15.01092\rho^2 + 327.62034\rho - 342.63126}{23.32347\rho^2 + 512.64565\rho - 532.36912} \quad (A.1)$$

According to the fitted equation shown in Fig. 6, we can easily obtain the reciprocal of average waiting time, namely the parameter $(1/\overline{W}_q)$, as shown in Eq. (A.2):

$$\frac{1}{\overline{W}_q} = 0.06094 - 0.06380\rho + \frac{0.00286}{\rho} \tag{A.2}$$

By substituting the corresponding parameter values (see Table 2) into Eq. (17), then combining the fitted equation shown in Fig. 5 and Eq. (16), the Eq. (17) becomes:

$$\delta = -\frac{0.14337\rho}{16.52292\rho^2 + 360.47717\rho - 377.14347} \tag{A.3}$$

By substituting the corresponding parameter values (see Table 2) into Eq. (16), then it becomes:

$$C_{Rn,L} = 66.04362 - \frac{11.65610\rho}{20.34\rho^2 + 443.93\rho - 464.27} \tag{A.4}$$

As shown in Eqs. (A.1)–(A.4), the parameters $\eta$, $(1/\overline{W}_q)$, $\delta$, and $C_{Rn,L}$ are closely dependent on utilization rate $\rho$.

## Appendix 2. Further description of queuing effect on shaft station radon concentration

To explain the linkage between the queuing of mine-cars and radon concentration in shaft station (particularly at the back end of shaft station), we assumed radon exhalation rate of uranium ore piles ($J_c$) and length of the shaft station ($L$) as variables, and the two parameters were assigned with greater values compared with their initial ones as shown in Table 2. Then, Eq. (16) becomes:

$$C_{Rn,L} = 64.8 + 11.82146 \times 10^{-3}L + 0.12195N_cJ_c \tag{A.5}$$

For convenience's sake, we further assumed sixteen cases (see Table A.1) for a supplemental description of mine-cars' queuing effect on shaft station radon concentration. Among these cases, the worst of conditions were taken into consideration, viz., the shaft station was occupied by awaiting mine-cars. According to the fitted equation shown in Fig. 5 and Eq. (A.5), the corresponding calculation results of utilization rate ($\rho$) and radon concentration at the back end of shaft station ($C_{Rn,L}$) were obtained (also see Table A.1).

**Table A.1**
Basic parameters and calculation results of the worst cases

| Case | $J_c$ (Bq·m$^{-2}$·s$^{-1}$) | $L$ (m) | $N_c$ [a] (=$2\overline{L}_q$) | $\rho$ | $C_{Rn,L}$ (Bq·m$^{-3}$) |
|---|---|---|---|---|---|
| 1 | 0.1 | 120 | 74 | 0.9471 | 67.1 |
| 2 | 0.1 | 150 | 92 | 0.9570 | 67.7 |
| 3 | 0.1 | 180 | 112 | 0.9644 | 68.3 |
| 4 | 0.1 | 210 | 120 | 0.9667 | 68.7 |
| 5 | 1.0 | 120 | 74 | 0.9471 | 75.2 |
| 6 | 1.0 | 150 | 92 | 0.9570 | 77.8 |
| 7 | 1.0 | 180 | 112 | 0.9644 | 80.6 |
| 8 | 1.0 | 210 | 120 | 0.9667 | 81.9 |
| 9 | 5.0 | 120 | 74 | 0.9471 | 111.3 |
| 10 | 5.0 | 150 | 92 | 0.9570 | 122.7 |
| 11 | 5.0 | 180 | 112 | 0.9644 | 135.2 |
| 12 | 5.0 | 210 | 120 | 0.9667 | 140.5 |
| 13 | 10.0 | 120 | 74 | 0.9471 | 156.5 |
| 14 | 10.0 | 150 | 92 | 0.9570 | 178.8 |
| 15 | 10.0 | 180 | 112 | 0.9644 | 203.5 |
| 16 | 10.0 | 210 | 120 | 0.9667 | 213.6 |

[a] $N_c$ is equal to the maximum even number lower than $(L/L_c)$, $L_c$ is shown in Table 2; the total number of mine-cars is 120.

As shown in Table A.1, with the increase of radon exhalation rate of uranium ore piles ($J_c$) and length of the shaft station ($L$), a rising tendency of radon station at the back end of shaft station has been noted. Specially, with respect to Case 15 and 16, shaft station radon concentration would be higher than the limited value (namely 200 Bq/m$^3$). However, only when uranium ore piles loaded in the awaiting mine-cars are wet enough and their grade and porosity are much greater than 0.11% and 2.5%, respectively, the equivalent radon exhalation rate of these ore plies may be reach 10 Bq/(m$^2$·s) or so.

## References


[1] UNSCEAR, Effects of Ionizing Radiation, United Nations Scientific Committee on the Effects of Atomic Radiation, 2006.
[2] L.A. Mehdipour, S.M.J. Mortazavi, E.B. Saion, H. Mozdarani, S.A. Aziz, H.M. Kamari, R. Faghihi, S. Mehdizadeh, M.R. Kardan, A. Mortazavi, M. Haghani, Natural ventilation considerations for radon prone areas of Ramsar, Iran J. Radiat. Res 12 (2014) 69–74.
[3] UNSCEAR, Sources and effects of ionizing radiation, United Nations Scientific Committee on the Effects of Atomic Radiation, 2000.
[4] G.M. Mudd, Radon sources and impacts: a review of mining and non-mining issues, Rev. Environ. Sci. Bio 7 (2008) 325–353.
[5] P. Sahu, D.P. Mishra, D.C. Panigrahi, V. Jha, R.L. Patnaik, Radon emanation from low-grade uranium ore, J. Environ. Radioact 126 (2013) 104–114.
[6] P. Sahu, D.P. Mishra, D.C. Panigrahi, V. Jha, R.L. Patnaik, N.K. Sethy, Radon emanation from backfilled mill tailings in underground uranium mine, J. Environ. Radioact 130 (2014) 15–21.
[7] P. Sahu, D.C. Panigrahi, D.P. Mishra, A comprehensive review on sources of radon and factors affecting radon concentration in underground uranium mines, Environ. Earth. Sci. 75 (2016) 1–19.
[8] COSTIND, Technical regulations for radon exhaustion and ventilation in underground uranium mine, Commission on Science, Technology and Industry for National Defense, 2006 (In Chinese).
[9] M.C. Mao, Analysis of emplacement condition of Dazhou uranium ore field, Ganhang ore belt and the prospecting direction of rich and large size uranium ore deposit here, Contrib. Geol. Miner. Resour. Res 17 (2002) 164–168 (In Chinese).
[10] M.C. Mao, Exploration key point, direction, target and task of Quzhou uranium resource base in Zhejiang province, Ur. Geol. 22 (2006) 350–355 (In Chinese).
[11] M. Laugna, J. Marklund, Business process modeling, simulation and design, Prentice Hall, Upper Saddle River, New Jersey, 2005.
[12] J. Sztrik, Basic queueing theory, University of Debrecen, Hungary, 2012.
[13] Y. Dodge, The concise encyclopedia of statistics, Springer New York, New York, 2008.
[14] J.L. Devore, Probability and statistics for engineering and the sciences, eighth ed., Duxbury Press, Boston, 2011.
[15] I. Miller, M. Miller, E. John, Freund's mathematical statistics, sixth ed., Prentice Hall, Upper Saddle River, New Jersey, 1999.
[16] C.L. Lu, Queuing theory, Beijing University of Posts and Telecommunications Press, Beijing, China, 2009 (In Chinese).
[17] M. Haviv, Queues—A course in queueing theory, Springer New York, New York, 2013.
[18] J.G. Allen, L.M. Zwack, D.L. MacIntosh, T. Minegishi, J.H. Stewart, J.F. McCarthy, Predicted indoor radon concentrations from a Monte Carlo simulation of 1000000 granite countertop purchases, J. Radiol. Prot 33 (2013) 151–162.
[19] V. Sundarapandian, Probability, statistics and queuing theory, PHI Learning Ltd, India, 2009.
[20] P. Furness, Applications of Monte Carlo simulation in marketing analytics, J. Direct Data Digit Mkt. Pract 13 (2011) 132–147.
[21] E. Zio, M. Marella, L. Podofillini, A Monte Carlo simulation approach to the availability assessment of multi-state systems with operational dependencies, Reliab. Eng. Syst. Safe 92 (2007) 871–882.
[22] Z.F. Wang, Y.T. Zheng, Mine fixed machinery and transport equipment, China University of Mining and Technology Press, Xuzhou, China, 2012 (In Chinese).
[23] C.H. Zhong, Y.C. Ding, Mine transport and hoist system, Chemical Industry Press, Beijing, China, 2013 (In Chinese).
[24] C.S. Hong, X.Y. Li, P.H. Hu, X.J. Li, Y.J. Ye, D. Xie, Study on regularity of radon and its daughter's concentration distribution in uranium mine shaft station, Nucl. Sci. Eng 35 (2015) 385–393 (In Chinese).
[25] G.Y. Zhao, C.S. Hong, X.Y. Li, C.P. Lin, P.H. Hu, Predictive analysis of shaft station radon concentrations in underground uranium mine: A case study, J. Environ. Radioact 158–159 (2016) 129–137.